PDE Estimation Techniques for Advanced Battery Management Systems - Part II: SOH Identification

S. J. Moura, N. A. Chaturvedi, and M. Krstić

***Abstract*— A critical enabling technology for electrified vehicles and renewable energy resources is battery energy storage. Advanced battery systems represent a promising technology for these applications, however their dynamics are governed by relatively complex electrochemical phenomena whose parameters degrade over time and vary across material design. Moreover, limited sensing and actuation exists to monitor and control the internal state of these systems. As such, battery management systems require advanced identification, estimation, and control algorithms. In this paper we examine state-of-health (SOH) estimation, framed as a parameter identification problem for parabolic PDEs and nonlinearly parameterized output functions. Specifically, we utilize the swapping identification method for unknown parameters in the diffusion partial differential equation (PDE). A nonlinear least squares method is applied to the output function to identify its unknown parameters. These identification algorithms are synthesized from the single particle model (SPM). In a companion paper we examine a new battery state-of-charge (SOC) estimation algorithm based upon the backstepping method for PDEs.**

I. INTRODUCTION

This paper examines identification algorithms for state-of-health (SOH) related parameters in advanced batteries described by partial differential equations (PDEs) with nonlinearly parameterized output functions.

A. Motivation & Technical Challenges

Reliable battery SOH estimation algorithms are of extreme importance due to their applications in electrified transportation [1] and energy storage systems for renewable sources [2]. The relevancy of this topic is further underscored by the 27.2 billion USD federal government investment in energy effciency and renewable energy research, including advanced batteries, under the American Recovery and Reinvestment Act (ARRA) of 2009 [3]. As such, battery management systems within these advanced transportation and energy infrastructures must have accurate knowledge of battery health [4]. Such knowledge enables them to efficiently route energy while satisfying power demands and device-level operating constraints [5].

Estimating battery SOH is particularly challenging for several reasons. First, no universally accepted definition for SOH exists. Some prevailing SOH-related metrics include charge capacity, internal impedance, and charge/discharge cycles. In this paper we frame SOH-estimation as a parameter estimation problem, where the estimated parameters are closely related to the mentioned SOH-metrics. A second challenge is that battery dynamics are governed by partial differential equations derived from electrochemical principles [6]. The only measurable quantities (voltage and current) are related to the states through nonlinear functions. Consequently we are dealing with infinite-dimensional plants with nonlinear output mappings. Designing parameter identification algorithms for such systems is highly nontrivial. Finally, directly measuring the states outside specialized laboratory environments [7] is impractical. This point means state and parameter estimation must be performed in tandem. On-going work addresses this third challenge via adaptive observers.

B. Literature Review

Long-term performance and health is a dominating theme throughout the battery science and engineering literature. One may divide this research into two categories: Offline and online identification methods.

Offline identification methods can vary from purely experimental techniques to specially designed algorithm designs. For example, experimental techniques may apply electrochemical, destructive structural testing, and various spectroscopy methods to determine the health of individual cells [8]. Multi-channel long-term battery cycling experiments attempt to relate various operating conditions (e.g. temperature, cycles, C-rate, depth of discharge, etc.) to cycle-life [9], [10]. Battery parameter identification algorithms, in contrast, study system identification algorithms for parameter identification from measured voltage, current, and temperature data [11].

Online identification techniques leverage various results from estimation and signal processing theory to determine battery SOH. Nearly all these studies utilize equivalent circuit models. Various algorithms have been investigated, including batch data reconciliation, moving-horizon parameter estimation [12], recursive least squares [13], bias-corrected least squares [14], impedance-based Kalman filters [15], extended Kalman filters [16], and particle filters [17]. The key advantage of these equivalent circuit model-based methods lie in their relatively low complexity. However, the state and parameter values correspond to phenomenological effects as opposed to the true physical values. Moreover, validation of these estimation algorithms is very difficult using in-situ methods [7].

This work was supported by the University of California Presidential Postdoctoral Fellowship Program and the National Science Foundation.

S. J. Moura and M. Krstic are with the Department of Mechanical and Aerospace Engineering and Cymer Center for Control Systems and Dynamics at the University of California, San Diego, CA 92093-0411, USA (e-mail: smoura@ucsd.edu; krstic@ucsd.edu)

N. A. Chaturvedi is with Robert Bosch LLC, Research & Technology Center, Palo Alto, CA 94304 USA (e-mail: nalin.chaturvedi@us.bosch.com)

C. Contributions

This paper augments the aforementioned research on battery SOH estimation by considering an *electrochemical-based PDE battery model*. Specifically, parameters in the PDE are identified using a swapping identification method. Parameters in the nonlinear output function are identified using a nonlinear least squares method. Consequently, this paper represents the first application of PDE parameter identification theory to electrochemical-based battery models.

D. Paper Organization

The paper is organized as follows: Section II summarizes the electrochemical-based single particle model used for parameter identification. Section III develops a swapping identification algorithm to determine unknown parameter which appear in the model's PDE and boundary conditions. Section IV develops a least-squares identification algorithm to determine unknown parameters which appear nonlinearly in the model's output function. Section V evaluates the performance of these identification algorithms via simulation studies. Finally, Section VI concludes the paper by summarizing its main results.

II. SINGLE PARTICLE MODEL

In this manuscript (and the companion paper on SOC estimation) we utilize the single particle model (SPM). The SPM concept was first applied to lithium battery systems in [18] where the key assumption is that the solid phase of each electrode can be idealized as a single spherical particle. In addition, the electrolyte concentration diffusion and migration dynamics are neglected and thermal effects are ignored. Mathematically, the model consists of two diffusion PDEs governing each electrode's concentration dynamics, where input current enters as a Neumann boundary condition. Output voltage is given by a nonlinear function of the state values at the boundary and the input current.

Indeed, this model captures less dynamic behavior than more complex electrochemical-based estimation models [18]. However, its structure is sufficiently simple for analyzing the stability and signal properties of the proposed identification algorithms - a key point of this work.

In order to provide some presentation completeness, yet not repeat information, we summarize the reduced SPM used for identification. In the companion paper on SOC estimation, a multi-PDE SPM is presented and its observability properties are analyzed. Since the SPM lacks complete observability, we reduce cathode diffusion to its equilibrium. Physical justification often exists for this reduction when the characteristic diffusion times are orders of magnitude less in the cathode than the anode. From this point, the radial and time dimensions are normalized and a coordinate transformation is performed to eliminate the first spatial derivative in the spherical diffusion PDE. The final result is a linear PDE (1)-(3) and nonlinear output equation (4)-(5) model used for identification purposes, shown below. Please refer to the companion article for more details on the SPM development.

$$\frac{\partial c}{\partial t}(r,t) = \varepsilon \frac{\partial^2 c}{\partial r^2}(r,t) \tag{1}$$

$$c(0,t) = 0 \tag{2}$$

$$\frac{\partial c}{\partial r}(1,t) - c(1,t) = -q\rho I(t) \tag{3}$$

where $\rho = R_s^- / (D_s^- F a^- A L^-)$.

$$\begin{aligned} V(t) = &\frac{RT}{\alpha^+ F} \sinh^{-1}\left(\frac{I(t)}{2a^+ A L^+ i_0^+(c_{ss}^+(t))}\right) \\ &- \frac{RT}{\alpha^- F} \sinh^{-1}\left(\frac{I(t)}{2a^- A L^- i_0^-(c_{ss}^-(t))}\right) \\ &+ U^+(c_{ss}^+(t)) - U^-(c_{ss}^-(t)) - R_f I(t) \end{aligned} \tag{4}$$

where

$$i_0^j(c_{ss}^j) = k^j \sqrt{c_e^0 c_{ss}^j(t)(c_{s,\max}^j - c_{ss}^j(t))}, j \in \{+,-\} \tag{5}$$

At least five parameters can be directly associated with battery SOH. These include the diffusion coefficient ε, boundary condition coefficient q, resistance R_f, and reaction rate coefficients k^+ and k^-.

In the remainder of this paper we divide the parameter identification algorithm into two separable parts. First, we design a swapping identifier to determine the unknown parameters ε and q in the PDE (1)-(3). Second, we consider a least squares algorithm to determine the unknown parameters R_f, k^+, k^- in the nonlinearly parameterized output function (4)-(5). Finally, simulation results demonstrate the performance of each algorithm. Throughout the development we shall assume full-state measurements. This intermediate step enables us to hopefully utilize the certainty equivalence principle to combine the state estimation techniques in the companion paper with the parameter identification algorithms below to form adaptive observers in future work.

III. PDE SWAPPING IDENTIFIER

The swapping identification technique follows a common parameter identification methodology for dynamic systems [19]. Namely, convert a dynamic parameterization of the plant into a static form by filtering the measured and regressor signals. Then apply gradient or least-squares estimation techniques to identify the parameters of this parametric model. We apply this methodology extended to parabolic PDE systems [20], where the filters are PDEs themselves and the adaptation laws involve inner products of continuous functions instead of matrix vectors.

To this end, consider the "estimation error" between the measured state $c(r,t)$ and filtered signals $\psi(r,t), \eta(r,t), \mu(r,t)$:

$$e = c - \varepsilon\psi - q\eta - \mu \tag{6}$$

where the static parametric model is $\varepsilon\psi + q\eta + \mu$. The variables ψ, η, μ are outputs of Kreisselmeier filters applied to the regressor signals. These filters are deliberately designed such that the PDE governing the estimation error $e(r,t)$ is exponentially stable. In particular, we select the following PDE for e:

$$\frac{\partial e}{\partial t}(r,t) = \hat{\varepsilon}\frac{\partial^2 e}{\partial r^2}(r,t) \tag{7}$$
$$e(0,t) = 0 \tag{8}$$
$$\frac{\partial e}{\partial r}(1,t) = -\frac{1}{2}e(1,t) \tag{9}$$

which one can easily show is exponentially stable using the Lyapunov function $V_{\text{lyap}}(t) = 1/2\int_0^1 e^2(r,t)dr$.

To obtain this PDE for the estimation error, the filters are designed as follows. The variable ψ is a filter corresponding to c_{rr}:

$$\frac{\partial \psi}{\partial t}(r,t) = \hat{\varepsilon}\frac{\partial^2 \psi}{\partial r^2}(r,t) + \frac{\partial^2 c}{\partial r^2}(r,t) \tag{10}$$
$$\psi(0,t) = 0 \tag{11}$$
$$\frac{\partial \psi}{\partial r}(1,t) = -\frac{1}{2}\psi(1,t) \tag{12}$$

η is the filter corresponding to the input current $I(t)$:

$$\frac{\partial \eta}{\partial t}(r,t) = \hat{\varepsilon}\frac{\partial^2 \eta}{\partial r^2}(r,t) \tag{13}$$
$$\eta(0,t) = 0 \tag{14}$$
$$\frac{\partial \eta}{\partial r}(1,t) = -\frac{1}{2}\eta(1,t) - \rho I(t) \tag{15}$$

and μ is the following filter

$$\frac{\partial \mu}{\partial t}(r,t) = \hat{\varepsilon}\frac{\partial^2 \mu}{\partial r^2}(r,t) - \hat{\varepsilon}\frac{\partial^2 c}{\partial r^2}(r,t) \tag{16}$$
$$\mu(0,t) = 0 \tag{17}$$
$$\frac{\partial \mu}{\partial r}(1,t) = -\frac{1}{2}\mu(1,t) + \frac{3}{2}c(1) \tag{18}$$

We now form the "parameter prediction error" as:

$$\hat{e} = c - \hat{\varepsilon}\psi - \hat{q}\eta - \mu \tag{19}$$

Using this parametric model, we implement the following gradient update laws with normalization:

$$\dot{\hat{\varepsilon}} = \gamma_\varepsilon \frac{\hat{\varepsilon}}{m^2}\cdot \text{Proj}_{\underline{\varepsilon}}\left\{\int_0^1 \hat{e}(r,t)\psi(r,t)dr\right\} \tag{20}$$
$$\dot{\hat{q}} = \gamma_q \frac{\hat{\varepsilon}}{m^2}\int_0^1 \hat{e}(r,t)\eta(r,t)dr \tag{21}$$
$$\text{where } m^2 = 1 + \|\psi\|^2 + \|\eta\|^2 \tag{22}$$

We use the projection operator to conserve the parabolic character of the system, namely $\hat{\varepsilon} \geq \underline{\varepsilon} > 0$. Note that the diffusion coefficient estimate $\hat{\varepsilon}$ shows up in the right-hand side of both update laws. This is unexpected, as nothing analogous is seen in parameter identification of finite-dimensional systems. As shown by the stability analysis below, however, this term helps ensure the boundedness of the parameter estimation error signals. A block diagram summarizing the swapping identifier is provided in Fig. 1

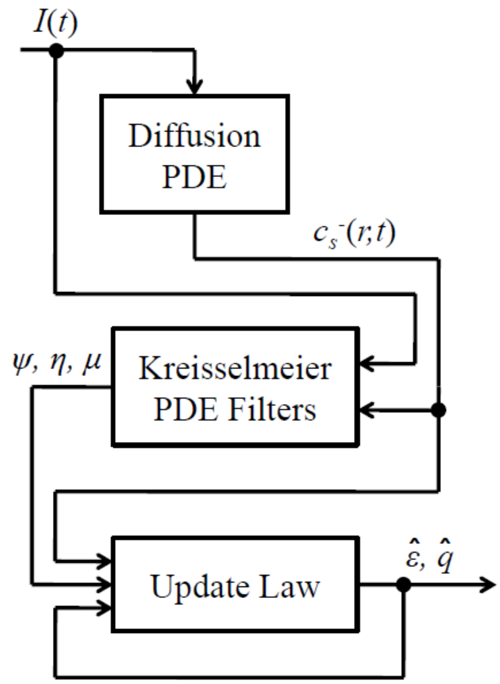

Fig. 1. Block diagram of the swapping identification algorithm for unknown parameters in the plant diffusion PDE, including the diffusion coefficient ϵ and boundary input coefficient q.

This identification scheme has the following signal properties:

$$\tilde{\varepsilon},\quad \tilde{q} \in \mathcal{L}_\infty \tag{23}$$
$$\dot{\hat{\varepsilon}},\quad \dot{\hat{q}} \in \mathcal{L}_2 \cap \mathcal{L}_\infty \tag{24}$$
$$\frac{\sqrt{\hat{\varepsilon}}}{m}\|\hat{e}\| \in \mathcal{L}_2 \cap \mathcal{L}_\infty \tag{25}$$

which can be shown using the following Lyapunov function:

$$V_{\text{lyap}}(t) = \frac{1}{2}\int_0^1 e^2(r,t)dr + \frac{1}{4\gamma_\varepsilon}\tilde{\varepsilon}(t)^2 + \frac{1}{4\gamma_q}\tilde{q}(t)^2 \tag{26}$$

which has the following derivative along the state trajectories:

$$\dot{V}_{\text{lyap}}(t) = \int_0^1 \hat{\varepsilon}ee_{rr}dr - \frac{\hat{\varepsilon}\tilde{\varepsilon}}{2m^2}\int_0^1 \hat{e}\psi dr - \frac{\hat{\varepsilon}\tilde{q}}{2m^2}\int_0^1 \hat{e}\eta dr \tag{27}$$
$$= -\frac{1}{2}\hat{\varepsilon}e(1)^2 - \hat{\varepsilon}\|e_r\|^2 + \frac{\hat{\varepsilon}}{2m^2}\int_0^1 \hat{e}edr - \frac{\hat{\varepsilon}}{2m^2}\|\hat{e}\|^2 \tag{28}$$

Applying the Cauchy-Schwarz, Poincaré, and Young's inequalities to the third term in the previous equation yields

$$\dot{V}_{\text{lyap}}(t) \leq -\frac{1}{2}\hat{\varepsilon}e(1)^2 - \frac{m^2-1}{m^2}\hat{\varepsilon}\|e_r\|^2 - \frac{\hat{\varepsilon}\|\hat{e}\|^2}{4m^2} \leq 0 \tag{29}$$

This gives us $\tilde{\varepsilon}, \tilde{q} \in \mathcal{L}_\infty$ and $\sqrt{\hat{\varepsilon}}\|\hat{e}\|/m \in \mathcal{L}_2$. These properties and (19) give us $\sqrt{\hat{\varepsilon}}\|\hat{e}\|/m \in \mathcal{L}_\infty$. Finally, the boundedness and square integrability of $\dot{\hat{\varepsilon}}$ and $\dot{\hat{q}}$ follow from the update laws (20)-(21).

Simulation results demonstrating this swapping identifier are presented in Section V.

IV. Parameter Identifier for Nonlinear Output Function

Next we develop an identification algorithm for the unknown parameters in the nonlinear output function. Recall that several unknown physical parameters related to SOH include R_f, k^+, k^-. With this in mind, we rearrange the output function in (4) to yield the following nonlinearly parameterized model:

$$z = \sinh^{-1}\left(\frac{\omega^+(t)}{a^+AL^+k^+\sqrt{c_e^0}}\right) - \sinh^{-1}\left(\frac{\omega^-(t)}{a^-AL^-k^-\sqrt{c_e^0}}\right) - \frac{\alpha F}{RT}R_f I(t) \tag{30}$$

where

$$z = \frac{\alpha F}{RT}\left[V(t) - U^+(c_{ss}^+(t)) + U^-(c_{ss}^-(t))\right] \tag{31}$$

$$\omega^+(t) = \frac{I(t)}{2\sqrt{c_{ss}^+(t)(c_{s,max}^+ - c_{ss}^+(t))}} \tag{32}$$

$$\omega^-(t) = \frac{I(t)}{2\sqrt{c_{ss}^-(t)(c_{s,max}^- - c_{ss}^-(t))}} \tag{33}$$

are signals that can be calculated from measured quantities and known parameters. Denote the unknown parameters by:

$$\theta = \begin{bmatrix} \theta_1 \\ \theta_2 \\ \theta_3 \end{bmatrix} = \begin{bmatrix} \left(a^+AL^+k^+\sqrt{c_e^0}\right)^{-1} \\ \left(a^-AL^-k^-\sqrt{c_e^0}\right)^{-1} \\ \frac{\alpha F}{RT}R_f \end{bmatrix} \tag{34}$$

Note that we have grouped together the SOH-related parameters (R_f, k^+, k^-) with known constants (F, R), measurable parameters (A, L^+, L^-, T), and empirical quantities (c_e^0, α). In practice this enables one to match the model to data when uncertainty exists among these non-SOH-related parameters. If their values are known, however, then R_f, k^+, k^- can be extracted.

In the following we develop an identification algorithm for this nonlinearly parameterized model which has local stability properties. The key idea is to (i) re-express the nonlinear model in terms of the parameter estimation error $\tilde{\theta}$, and (ii) perform a Taylor Series expansion around $\tilde{\theta} = 0$. To this end we begin with the nonlinear parametric model

$$z = \sinh^{-1}(\theta_1\omega^+) - \sinh^{-1}(\theta_2\omega^-) - \theta_3 I \tag{35}$$

which expressed in terms of $\tilde{\theta}$ is

$$z = \sinh^{-1}\left[(\hat{\theta}_1 + \tilde{\theta}_1)\omega^+\right] - \sinh^{-1}\left[(\hat{\theta}_2 + \tilde{\theta}_2)\omega^-\right] - \left[(\hat{\theta}_3 + \tilde{\theta}_3)\right] I \tag{36}$$

Then the Taylor series expansion of this equation around $\tilde{\theta} = 0$ is given by:

$$z = \sinh^{-1}(\hat{\theta}_1\omega^+) - \sinh^{-1}(\hat{\theta}_2\omega^-) - \hat{\theta}_3 I \quad \left(1 + \hat{\theta}_1^2{\omega^+}^2\right)^{-1/2}\omega^+\tilde{\theta}_1 - \left(1 + \hat{\theta}_2^2{\omega^-}^2\right)^{-1/2}\omega^-\tilde{\theta}_2 - I\tilde{\theta}_3 + \mathcal{O}(\tilde{\theta}^T\tilde{\theta}) \tag{37}$$

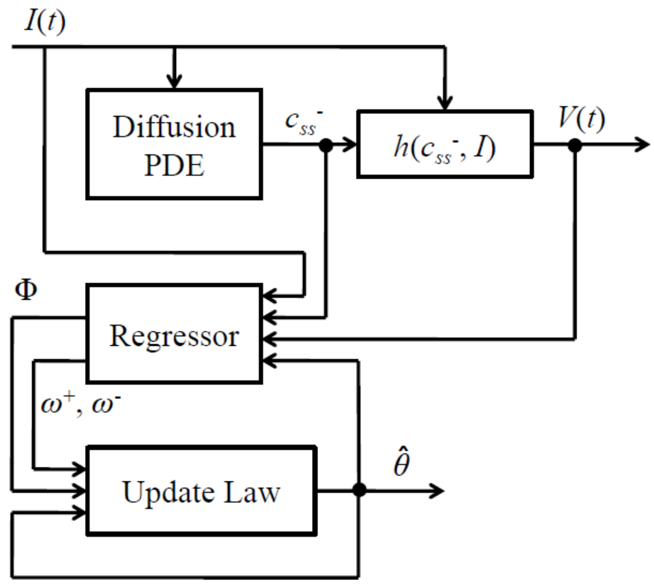

Fig. 2. Block diagram of the nonlinear least-squares identification algorithm for unknown parameters in the plant output function.

Rearranging terms we get

$$z - \sinh^{-1}(\hat{\theta}_1\omega^+) + \sinh^{-1}(\hat{\theta}_2\omega^-) + \hat{\theta}_3 I = \tilde{\theta}^T\Phi + \mathcal{O}(\tilde{\theta}^T\tilde{\theta}) \tag{38}$$

where

$$\Phi = \begin{bmatrix} \left(1 + \hat{\theta}_1^2{\omega^+}^2\right)^{-1/2} \\ -\left(1 + \hat{\theta}_2^2{\omega^-}^2\right)^{-1/2} \\ -I \end{bmatrix} \tag{39}$$

is the regressor vector, which depends upon measured signals and parameter estimates only.

We now choose a least-squares parameter update law as follows:

$$\dot{\hat{\theta}} = P e_{nl}\Phi \tag{40}$$

$$\dot{P} = -P\frac{\Phi\Phi^T}{m^2}P, \qquad P(0) = P_0 = P_0^T > 0 \tag{41}$$

where $e_{nl} = z - \sinh^{-1}(\hat{\theta}_1\omega^+) + \sinh^{-1}(\hat{\theta}_2\omega^-) + \hat{\theta}_3 I$ is the estimation error for the nonlinear model and $m^2 = 1 + \gamma\Phi^T\Phi$ is the normalization signal. A block diagram summarizing the nonlinear least-squares update method is shown in Fig. 2

The stability properties of the parameter adaptation law (40)-(41) can be studied by following the ideas presented in the adaptive law design of [21]. Specifically, consider the estimation error dynamics

$$\dot{\tilde{\theta}} = P\frac{\Phi\Phi^T}{m^2}\tilde{\theta} + P\frac{\Phi}{m^2}\mathcal{O}(\tilde{\theta}^T\tilde{\theta}) \tag{42}$$

The first term on the right-hand side provides a stabilizing effect while the remaining terms are potentially destabilizing. Local stability may be established using the results for linear time-varying systems and linearization in Section 4.6 of

Khalil [22]. Namely, one may linearize the estimation error dynamics and consider the associated Lyapunov function $V_{\text{lyap}} = \frac{1}{2}\tilde{\theta}^T P^{-1}\tilde{\theta}$. If the regressor signals are bounded, then the derivative of V_{lyap} along the trajectories of $\tilde{\theta}$ is strictly negative definite in $\|\tilde{\theta}\|$ under an appropriate persistence of excitation condition for the regressor Φ.

V. SIMULATION STUDIES

Next we examine the PDE swapping and output function identifiers through simulation. Throughout these simulations we work in normalized (r, t) coordinates. This means each normalized time unit is equivalent to 745 sec and the particle surface is at $r = 1$. We utilize the model parameters from [11] and apply the finite central difference method within our solver schemes. We also apply the same current input trajectory used to study the state estimation problem in the companion manuscript and apply zero mean, 2 mV standard deviation, normally distributed noise to the measured voltage.

A. PDE Swapping Identifier

Due to the normalization procedure the true diffusion and boundary coefficient parameters are $\varepsilon = q = 1$. In Figure 3 we demonstrate results for the swapping identifier. The initial diffusion and boundary coefficients are set to $\hat{\varepsilon}(0) = 5$ and $\hat{q}(0) = 0$, respectively. The filters are initialized as follows: $\psi(r, 0) = \eta(r, 0) = 0, \forall r \in [0, 1]$ and $\mu(r, 0) = r \cdot c_s^-(r, 0)$.

As shown by Fig. 3, the swapping identifier estimates converge close to the true values, where the exit estimates are: $\hat{\varepsilon}(1.5) = 1.0042$ and $\hat{q}(1.5) = 0.9815$. To further provide insight into the swapping identifier, Fig. 4 portrays the evolution of the prediction error $\hat{e}(r, t)$ defined in (19), over the time interval $t \in [0.1, 0.6]$. The gradient update laws force this spatially distributed error signal to zero.

B. Parameter Identifier for Nonlinear Output Function

Next we discuss simulation results for the nonlinear least-squares identifer for SOH-related parameters in the output function (4)-(5). The parameter estimates are incorrectly initialized as follows: $\hat{\theta}(0) = [0.75\theta_1, 2\theta_2, 3\theta_3]^T$. Figure 5(a) shows the evolution of the algorithm parameter estimates. The corresponding SOH-related parameters (R_f, k^+, k^-) are displayed in Fig. 5(b)-(c). In all cases, one can see that the estimates converge near the true values. The existence of some parameter bias is an expected characteristic of nonlinear least squares estimators. In this case, a parameter sensitivity analysis [23] reveals linear dependence between parameters - thus producing bias. The impact of these parameter estimates on voltage can be seen in Fig. 6(a) and (b), where the estimated voltage quickly converges to the estimated value after the first non-zero current input is applied.

VI. CONCLUSION

This paper examines PDE and nonlinear parameter identification techniques for battery state-of-health estimation. Unlike most existing SOH estimation studies, we utilize an electrochemical-based single particle model for identification. The parameter identification process is separated into two parts. First, a PDE swapping identifier determines the unknown diffusion and boundary control input coefficients. Stability and signal properties are analyzed for this identifier. Second, a nonlinear least squares method is applied to determine unknown parameters in the nonlinearly parameterized output function. Performance attributes are evaluated through simulation studies.

A key assumption throughout this work is the availability of full-state measurements. On-going work relaxes this assumption by formulating a parametric model which uses measured signals only. This enables the formulation of an adaptive observer which simultaneously estimates states (SOC) and parameters (SOH). We also aim to analyze the composed state estimator/parameter identifier structure and evaluate its performance theoretically and experimentally.

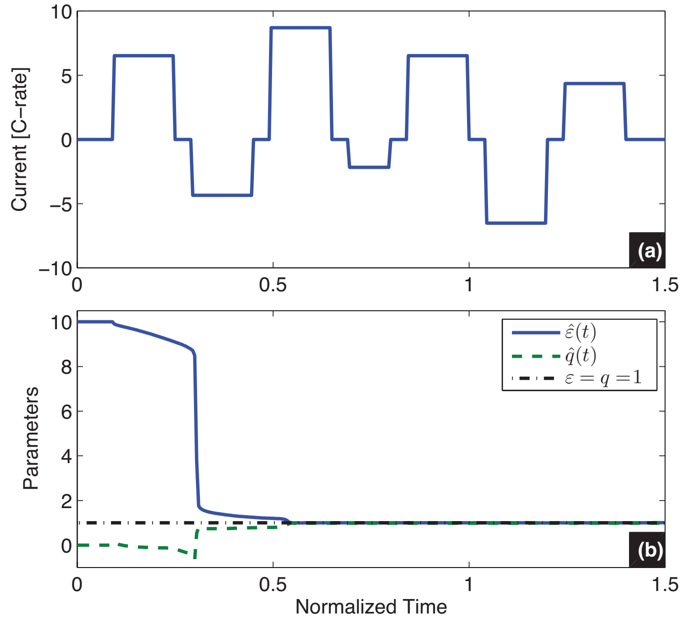

Fig. 3. The input current (a) and parameter estimates (b) for the swapping identifier (diffusion coefficient, $\hat{\varepsilon}$; boundary input coefficient, $\hat{q}$). The true parameter values are both equal to one.

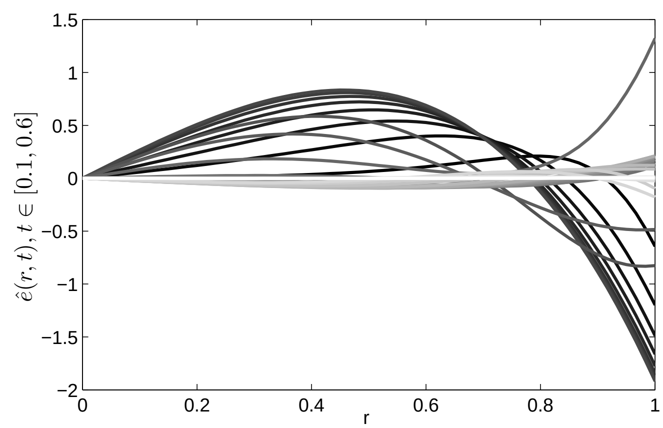

Fig. 4. Evolution of the parameter prediction error $\hat{e}(r, t)$ defined in (19), over the time interval $t \in [0.1, 0.6]$. As time proceeds, the curves get lighter in shade and converge to the origin.

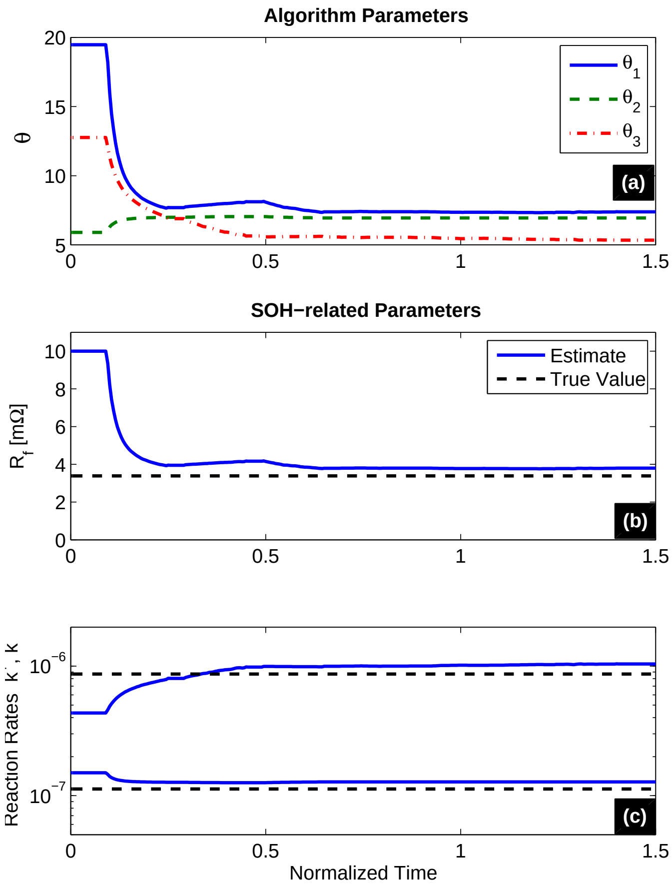

Fig. 5. Evolution of the algorithm parameter estimates (a) and SOH-related parameter estimates (b)&(c). True values for the SOH-related parameters are shown in (b)&(c).

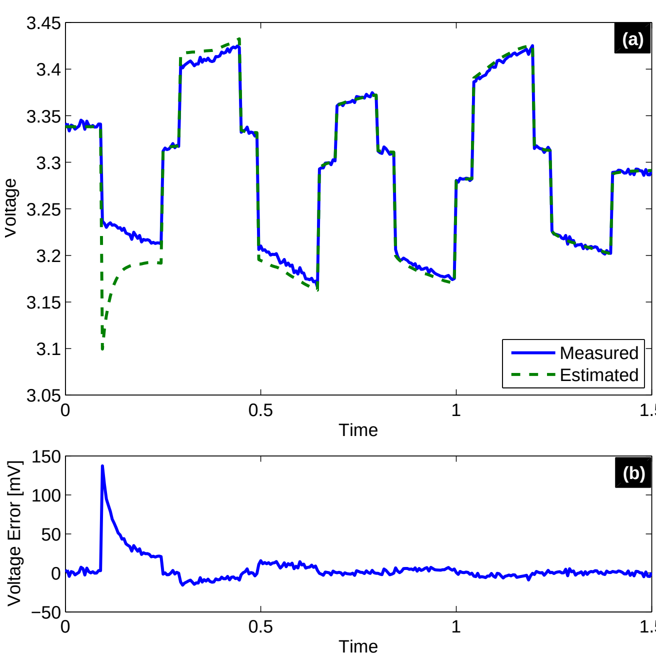

Fig. 6. The top plot (a) portrays measured and estimated voltage. The bottom plot (b) demonstrates the voltage error.

REFERENCES

[1] L. Burns, J. McCormick, and C. Borroni-Bird, "Vehicle of change," *Scientific American*, vol. 287, no. 4, pp. 40–49, 2002.

[2] P. Denholm, E. Ela, B. Kirby, and M. Milligan, "Role of energy storage with renewable electricity generation," National Renewable Energy Laboratory (NREL), Golden, CO., Tech. Rep. Technical Report NREL/TP-6A2-47187, 2010.

[3] D. Obey, "American Recovery and Reinvestment Act of 2009," Feb. 2009, Public Law No: 111-5. [Online]. Available: http://frwebgate.access.gpo.gov/

[4] N. A. Chaturvedi, R. Klein, J. Christensen, J. Ahmed, and A. Kojic, "Algorithms for advanced battery-management systems," *IEEE Control Systems Magazine*, vol. 30, no. 3, pp. 49 – 68, 2010.

[5] S. J. Moura, "Techniques for Battery Health Conscious Power Management via Electrochemical Modeling and Optimal Control," Ph.D. dissertation, University of Michigan, Ann Arbor, 2011.

[6] K. Thomas, J. Newman, and R. Darling, *Advances in Lithium-Ion Batteries*. New York, NY USA: Kluwer Academic/Plenum Publishers, 2002, ch. Mathematical modeling of lithium batteries, pp. 345–392.

[7] J. B. Siegel, X. Lin, A. G. Stefanopoulou, D. S. Hussey, D. L. Jacobson, and D. Gorsich, "Neutron imaging of lithium concentration in LFP Pouch cell battery," *Journal of the Electrochemical Society*, vol. 158, no. 5, pp. A523 – A529, 2011.

[8] P. Liu, J. Wang, J. Hicks-Garner, E. Sherman, S. Soukiazian, M. Verbrugge, H. Tataria, J. Musser, and P. Finamore, "Aging Mechanisms of LiFePO4 Batteries Deduced by Electrochemical and Structural Analyses," *Journal of the Electrochemical Society*, vol. 157, no. 4, pp. A499–A507, 2010.

[9] J. Wang, P. Liu, J. Hicks-Garner, E. Sherman, S. Soukiazian, M. Verbrugge, H. Tataria, J. Musser, and P. Finamore, "Cycle-life model for graphite-LiFePO4 cells," *Journal of Power Sources*, vol. 196, no. 8, pp. 3942 – 3948, 2011.

[10] S. B. Peterson, J. Apt, and J. Whitacre, "Lithium-ion battery cell degradation resulting from realistic vehicle and vehicle-to-grid utilization," *Journal of Power Sources*, vol. 195, no. 8, pp. 2385 – 2392, 2010.

[11] J. C. Forman, S. J. Moura, J. L. Stein, and H. K. Fathy, "Parameter Identification of the Doyle-Fuller-Newman Model Based on Experimental Cycling of a Li-ion LiFePO4 Battery Using a Genetic Algorithm," *2011 American Control Conference*, 2011.

[12] E. Gatzke, A. Stamps, C. Holland, and R. White, "Analysis of capacity fade in a lithium ion battery," *Journal of Power Sources*, vol. 150, pp. 229–39, 10/04 2005.

[13] M. Verbrugge and E. Tate, "Adaptive state of charge algorithm for nickel metal hydride batteries including hysteresis phenomena," *Journal of Power Sources*, vol. 126, no. 1-2, pp. 236–249, 2004.

[14] M. Sitterly, L. Y. Wang, G. G. Yin, and C. Wang, "Enhanced identification of battery models for real-time battery management," *IEEE Trans. on Sustainable Energy*, vol. 2, no. 3, pp. 300 – 308, 2011.

[15] D. V. Do, C. Forgez, K. El Kadri Benkara, and G. Friedrich, "Impedance observer for a Li-ion battery using Kalman filter," *IEEE Transactions on Vehicular Technology*, vol. 58, no. 8, pp. 3930 – 3937, 2009.

[16] G. L. Plett, "Extended Kalman filtering for battery management systems of LiPB-based HEV battery packs. Part 3. State and parameter estimation," *J. of Power Sources*, vol. 134, no. 2, pp. 277–92, 2004.

[17] B. Saha, K. Goebel, S. Poll, and J. Christophersen, "Prognostics methods for battery health monitoring using a bayesian framework," *Instrumentation and Measurement, IEEE Transactions on*, vol. 58, no. 2, pp. 291 –296, Feb 2009.

[18] S. Santhanagopalan, Q. Guo, P. Ramadass, and R. E. White, "Review of models for predicting the cycling performance of lithium ion batteries," *Journal of Power Sources*, vol. 156, no. 2, pp. 620 – 628, 2006.

[19] P. Ioannou and J. Sun, *Robust Adaptive Control*. Prentice-Hall, 1996.

[20] M. Krstic and A. Smyshlyaev, "Adaptive control of PDEs," *Annual Reviews in Control*, vol. 32, no. 2, pp. 149–60, 12 2008.

[21] M. Krstic and A. Banaszuk, "Multivariable adaptive control of instabilities arising in jet engines," *Control Engineering Practice*, vol. 14, no. 7, pp. 833 – 42, 2006.

[22] H. K. Khalil, *Nonlinear Systems*, 3rd ed. Prentice Hall, 2002.

[23] B. F. Lund and B. A. Foss, "Parameter ranking by orthogonalization - Applied to nonlinear mechanistic models," *Automatica*, vol. 44, no. 1, pp. 278 – 281, 2008.